Int. J. Electrochem. Sci., 11 **(2016)** 2954 - 2961

International Journal of
ELECTROCHEMICAL
SCIENCE
www.electrochemsci.org

MoS_2 Flowers Grown on Graphene/Carbon Nanotubes: a Versatile Substrate for Electrochemical Determination of Hydrogen Peroxide

Mani Govindasamy, Veerappan Mani[1,2], Shen-Ming Chen[1,], Raj Karthik[1], Kesavan Manibalan[1], Rajaji Umamaheswari[3]*

[1]Department of Chemical Engineering and Biotechnology, National Taipei University of Technology, No.1, Section 3, Chung-Hsiao East Road , Taipei 106, Taiwan
[2]Institute of Biochemical and Biomedical Engineering, National Taipei University of Technology, No.1, Section 3, Chung-Hsiao East Road , Taipei 106, Taiwan
[3]Department of Chemistry, St. Joseph's College (Autonomous), Tiruchirappalli-620 002, Tamil Nadu, India
[*]E-mail: smchen78@ms15.hinet.net

Received: 20 January 2016 / *Accepted:* 12 February 2016 / *Published:* 1 March 2016

Flower-like MoS_2 nanostructure was grown on graphene and carbon nanotubes (GR-MWCNTs) via *in-situ* hydrothermal method and the resulting composite was employed for determination of hydrogen peroxide (H_2O_2). The MoS_2/GR-MWCNTs composite was characterized by scanning electron microscopy, Energy-dispersive X-ray spectroscopy and electrochemical methods. MoS_2/GR-MWCNTs possess three dimensional nanostructure, large electrochemically active surface area, porosity, and high conductivity and it was used for the enzymeless electrochemical determination of hydrogen peroxide. MoS_2/GR-MWCNTs composite film modified electrode showed excellent electrocatalytic ability to the reduction of H_2O_2. The composite delivered significantly improved electrocatalytic ability to H_2O_2 in comparison with control electrodes. Furthermore, the electrode exhibited low overpotential, high faradaic current and fast response time. MoS_2/GR-MWCNTs composite film modified electrode responds quickly to H_2O_2 over wide working concentration range of 5 μM–145 μM, sensitivity of 5.184 μAμM cm^{-2} and detection limit of 0.83 μM. Moreover, the sensor exhibited appreciable stability, repeatability and reproducibility. Real-time application was demonstrated in biological sample which showed good recoveries. The other advantages of the fabricated biosensor are simple and green fabrication approach, roughed and stable electrode surface, fast in sensing and highly reproducible, good biocompatibility, electrocatalytic ability and excellent synergy between MoS_2, MWCNTs and GR.

Keywords: two dimensional layered materials, MoS_2, Graphene, MWCNTs, electrochemical sensor, hydrogen peroxide, and electrocatalysis

1. INTRODUCTION

Layered 2D transition metal dichalcogenides, such as MoS_2, WS_2, MoSe2, WSe2 etc., have received considerable interest in recent year [1]. Recent studies revealed that the electronic structure of nano-sized MoS_2 is similar to platinum and hence it has great potential to be as sustainable non-platinum catalyst in catalysis [2, 3]. Engineering advanced nanocomposites by hybridization of two or more materials is the most promising way to overcome the shortcomings of individual components and to develop advanced materials for specific applications [4]. Graphene nanosheets (GR) and multiwalled carbon nanotubes (MWCNTs) are two widely acclaimed carbon nanomaterials to prepare functionalized hybrid nanostructures [4]. Our previous studies indicated that GR and MWCNTs hybrid (GR-MWCNTs) three dimensional nanoarchitectures is ideal building blocks to fabricate interesting hybrid materials which can also preserve the individual properties [5-8]. Till now, several MoS_2 functionalized graphene materials with different structures were developed which were shown promising applications in hydrogen evolution [2, 9], photovoltaics [10], lithium-ion batteries [11], and supercapacitors [12]. Despite the interesting attributes of MoS_2 functionalized carbon nanostructures, they were hardly explored in electrochemical sensor applications. Significant efforts have been made to develop novel MoS_2 nanostructures such as, nanosheets [13], nanoplates [14] and nanospheres [15]. Recently, MoS_2 flowers and nanoflowers were prepared for hydrogen evolution reaction [16], supercapacitors [17], lithium ion batteries [18] and dye-sensitized solar cells [19].

H_2O_2 is a vital constituent of plant tissues and regulates the plant metabolism, acclamatory processes and gene expressions [5, 20, 21]. In addition, it has excellent antiseptic and anti-bacterial properties. Also, it is widely used in industries as oxidizing, antibacterial and bleaching agents. Therefore, a sensitive and selective determination platform is necessary for the quantitative determination of H_2O_2 in clinical and industrial analysis [22]. Designing advanced multi-dimensional GR-MWCNTs hybrid structures for electrochemical sensors, biosensors and energy applications is our lab's continuous research interest [5, 8, 23, 24]. Herein, we have synthesized and characterized the MoS_2 flowers decorated GR-MWCNTs nanostructure and employed electrochemical sensing of H_2O_2. The nanostructure was prepared via *in-situ* one pot hydrothermal synthesis and employed in sensitive and selective determination of H_2O_2. The 3D hierarchical network of MoS_2/GR-MWCNTs hybrid is composed of 2D GR and MoS_2 and 1D MWCNTs nanostructures. The main objective of the present work is to prepare MoS_2/GR-MWCNTs hybrid for the sensitive and selective determination of H_2O_2. The nanocomposite film modified electrode exhibited excellent electrocatalytic ability to reduce H_2O_2 with wide linear range, low limit of detection and high sensitivity. The preparation of the nanocomposite is simple, reproducible without required any hazardous reducing agents. The GR-MoS_2 film modified electrode possesses high electrochemically active surface area, porous and roughed surfaces, high conductivity, large edge plane sites and good biocompatibility.

2. EXPERIMENTAL

2.1 Chemicals and Apparatus

Graphite (powder, < 20 μm), MWCNTs (bundled > 95%, O.D×I.D×length = 7–15×3–6×0.5–200 μm), sodium molybdate ($Na_2MoO_4.2H_2O$), and all other reagents including solvents were

purchased from Sigma-Aldrich and used as received. All the electrochemical measurements were carried out using CHI 1205A electrochemical work station (CH Instruments, Inc., U.S.A) at ambient temperature. Electrochemical studies were performed in a conventional three electrode cell using modified glassy carbon electrode (GCE) (Bioanalytical Systems, Inc., USA) as a working electrode (area 0.071 cm^2), saturated Ag|AgCl (saturated KCl) as a reference electrode and Pt wire as a counter electrode. Prior to each electrochemical experiment, the electrolyte solutions were deoxygenated with pre-purified nitrogen for 15 min unless otherwise specified. The supporting electrolyte used for the electrochemical studies was 0.05 M phosphate buffer (pH 7) prepared from sodium dihydrogen phosphate and disodium hydrogen phosphate.

Amperometric measurements were performed with analytical rotator AFMSRX (PINE instruments, USA) with a rotating disc electrode (RDE) having working area of 0.21 cm^2. Scanning electron microscopy (SEM) and Energy-dispersive X-ray (EDX) spectra were performed using Hitachi S-3000 H scanning electron microscope and HORIBA EMAX X-ACT (Sensor + 24V=16 W, resolution at 5.9 keV) respectively.

2.2 Synthesis of MoS_2/GR-MWCNTs and electrode fabrication

Graphite oxide was prepared from graphite by Hummers method and exfoliated to graphene oxide (GO) in water via ultrasonic agitation for 2 h [25]. Then, the GO dispersion was subjected to centrifugation for 30 min at 4000 rpm to remove unexfoliated graphite oxide. Next, 20 mg MWCNTs was added into 20 ml GO (1 mg mL^{-1}) dispersion (GO/MWCNTs; w/w=1/1) and ultrasonicated for 2 h at room temperature [7]. The unstabilized MWCNTs and excess GO were removed by subjecting two successive centrifugation cycles (30 min each) at 8000 rpm and 14000 rpm, respectively. The black color sediment (GO-MWCNTs) was washed with water (60 mL) and ethanol (6 mL) respectively and overnight dried. Next, 25 mg GO-MWCNTs powder was re-dispersed in 100 mL water (1 mg mL^{-1}) via ultrasonication for 30 min. Then, 180 mg $Na_2MoO_4.2H_2O$ and 350 mg thiourea were added successively and stirred with magnetic stirrer for 30 min [18]. Next, the whole reaction mixture was transferred to a Teflon-lined autoclave and heated to 200°C for 24 h. The black sediment was centrifuged, washed with copious amount of water and ethanol (each washing 2 times) successively and vacuum dried in oven at 80°C for overnight. The MoS_2/GR-MWCNTs composite (1 mg mL^{-1}) was redispersed in water/ethanol (v/v%; 40/60%) solvent mixture through ultrasonication for 30 min. Meanwhile, individual GR-MoS_2 and MWCNTs-MoS_2 were prepared separately by following similar procedure.

GCE surface was polished with 0.05 μm alumina slurry using a Buehler polishing kit, then washed with water and dried. 6 μl MoS_2/GR-MWCNTs dispersion was dropped at the pre-cleaned GCE and dried at room temperature. As control, MoS_2/GR and MoS_2/MWCNTs film modified GCEs were prepared.

3. RESULTS AND DISCUSSION

3.1 Characterization of MoS_2/GR-MWCNTs

The SEM image of GR-MoS_2 portrays thin GR sheets along with tubular networks of MWCNTs (Fig. 1A). The SEM image of MoS_2/GR depicts typical wrinkled sheet like morphology characteristics of GR and MoS_2 two dimensional sheets. The sheet thickness varies in nanometers, while length of the sheets ranging in micrometer as expected for GR sheets. EDX analysis was performed in order to confirm the elements. EDX spectrum of GR-MoS_2 (Fig. 1C) shows the signals corresponding to carbon, molybdenum and sulfur signals with weight percentages of 51.1, 12.68 and 36.21 respectively, while corresponding atomic percentages were 84.63, 7.87 and 7.51% respectively. The SEM image of MoS_2/GR-MWCNTs (Fig. 1B) shows interesting morphology, wherein flower-like MoS_2 were uniformly grown on the three dimensional interconnected hierarchical network. Besides, the SEM image shows the presence of high surface area, large wrinkled sites for catalysis and uniformity. Notably, MoS_2/GR unable to form flower structure and hence the flower formation mechanism in MoS_2/GR-MWCNTs composite should be originated from MWCNTs. As evident from the SEM image, MWCNTs are the building blocks to form MoS_2 flowers. In addition, they are acting as conducting wires to connect all the networks of flowers which facilitated good conductivity. EDX spectrum of MoS_2/GR-MWCNTs (Fig. 1D) shows the signals corresponding to carbon, molybdenum and sulfur signals with weight percentages of 61.48, 12.87 and 25.65 respectively, while corresponding atomic percentages were 88.45, 6.93 and 4.62% respectively.

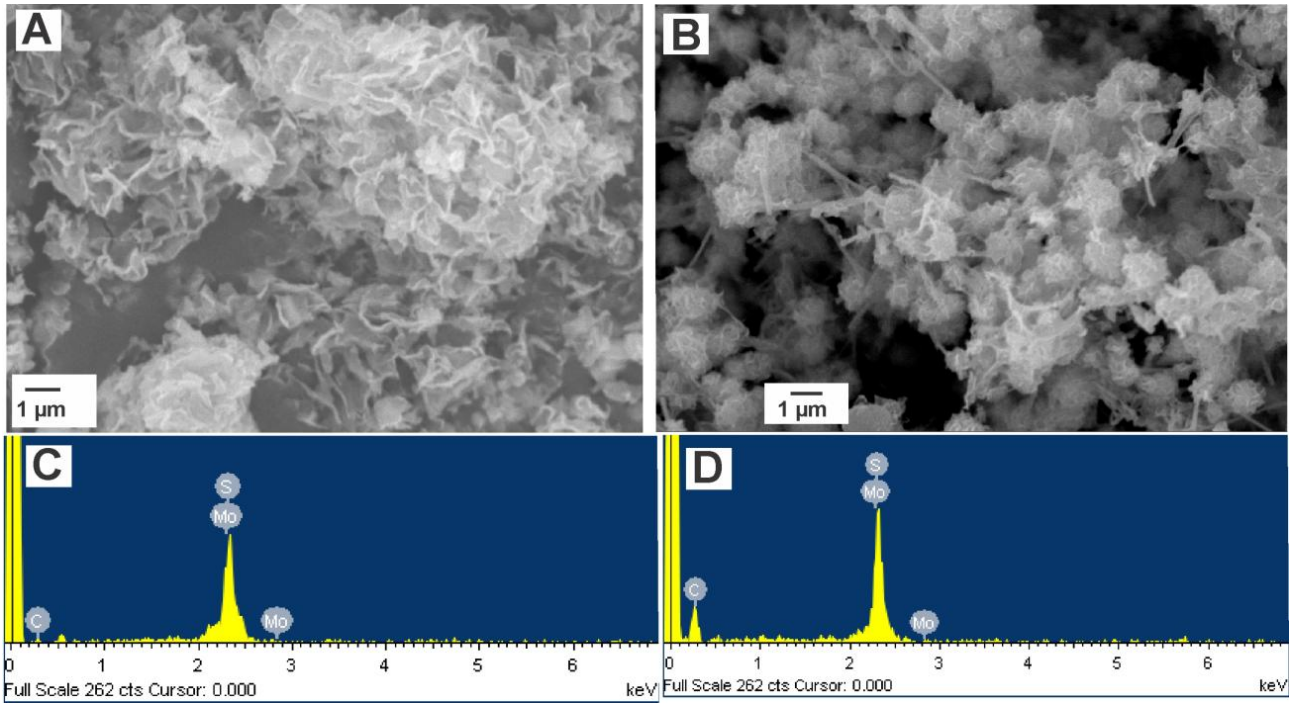

Figure 1. SEM images of MoS_2/GR (A) and MoS_2/GR-MWCNTs (B). EDX spectra of MoS_2/GR (C) and MoS_2/GR-MWCNTs (D)

3.2 Electrocatalytic reduction of H_2O_2

Fig. 2A displays the cyclic voltammograms (CVs) obtained at MoS_2/MWCNTs (a), MoS_2/GR (b), and MoS_2/GR-MWCNTs films modified electrode in phosphate buffer (pH 7) containing 1 mM H_2O_2. The scan rate was hold at 50 mV s^{-1}. The electrocatalytic ability of these modified electrodes was in the following order: MoS_2/GR-MWCNTs>MoS_2/GR >MoS_2/MWCNTs. The MoS_2/GR-MWCNTs exhibited highly enhanced electrocatalytic ability to reduce H_2O_2 which is obvious from the observed high faradaic current and less overpotential. Highly enhanced anodic peak current (I_{pa}) and low overpotential observed for the reduction of H_2O_2 at MoS_2/GR-MWCNTs film indicates fast electron transfer kinetics and promising electrocatalytic ability of the prepared film. The control electrodes (MoS_2/GR and MoS_2/MWCNTs) had shown comparatively less electrocatalytic ability than the MoS_2/GR-MWCNTs. The outstanding electrocatalytic ability of MoS_2/GR-MWCNTs can be manifested to the great synergetic effect between MoS_2, GR and MWCNTs [26]. GR-MWCNTs are suitable matrix for the high loading of catalytically active MoS_2 by providing anchoring sites. In addition, GR-MWCNTs possess numerous edge planes like defects which enabled additional catalytic sites to access H_2O_2. Fig. 2B shows the CVs obtained at MoS_2/GR-MWCNTs/GCE in phosphate buffer (pH 7) containing 1 mM H_2O_2 at different scan rates. As shown in figure, the cathodic peak current responsible for reduction of H_2O_2 linearly increases as the scan rate increases, indicated the occurrence of surface confined H_2O_2 reduction at MoS_2/GR-MWCNTs film. Fig. 2C presents the CVs obtained at MoS_2/GR-MWCNTs/GCE in presence of various concentrations of H_2O_2 in phosphate buffer (pH 7). The cathodic peak increases linearly as the concentration of H_2O_2 increases. For voltammetric detection, the linear concentration range is observed from 1–5 mM.

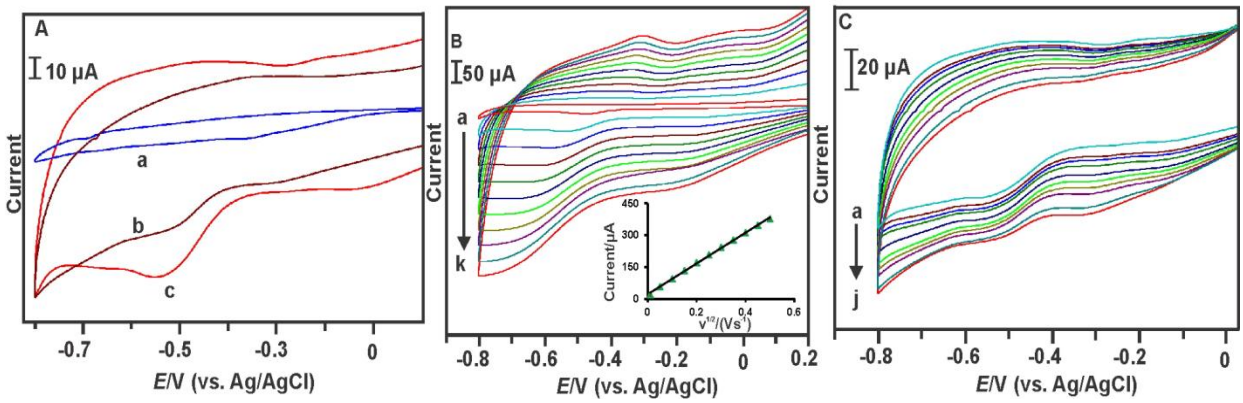

Figure 2. (A) Cyclic voltammograms obtained at GR/MWCNTs (a), MoS_2/GR (b), MoS_2/GR-MWCNTs (c) films modified GCE in phosphate buffer (pH 7) containing 1 mM H_2O_2 at the scan rate of 50 mVs^{-1}. (B) Cyclic voltammograms obtained at MoS_2/GR-MWCNTs film modified GCE in phosphate buffer (pH 7) containing 1 mM H_2O_2 at different scan rates; a=0.01, b=0.05, c=0.1, d=0.15, e=0.2, f= 0.25, g= 0.3, h= 0.35, i= 0.4, j=0.45 and k= 0.5 Vs^{-1}). Inset: plot of current vs. $v^{1/2}$. (C) Cyclic voltammograms obtained at MoS_2/GR-MWCNTs film modified GCE in phosphate buffer (pH 7) containing different concentrations of H_2O_2 (a=0, b=0.1, c=0.2, d=0.3, e=0.4, f= 0.5, g= 0.6, h= 0.7, i= 0.8 and j=0.9).

3.3 Amperometric detection of H_2O_2

Fig. 3A displays the amperogram obtained at MoS_2/GR-MWCNTs film modified RDE for sequential injection of H_2O_2 at regular intervals (50 s) into continuously stirred phosphate buffer (pH 7). The applied electrode potential (E_{app}) was hold at – 0.45 V, while rotation speed was fixed at 1500 rpm. Rapid and well defined responses were observed for each addition. The amperometric responses were linearly increased in the concentration range of 5 μM–145 μM. A plot between [H_2O_2] and I_p exhibits good linearity (Fig. 3B). Sensitivity and detection limit of the sensor were calculated to be 5.184 μAμM cm^{-2} and 0.83 μM respectively. The LOD of the sensor was calculated by using the formula, LOD= 3 s_b/S (where, s_b =standard deviation of blank signal and S =sensitivity) [27]. The important analytical parameters such as detection limit, linear range and sensitivity were quite comparable with previous reports [20, 28-31].

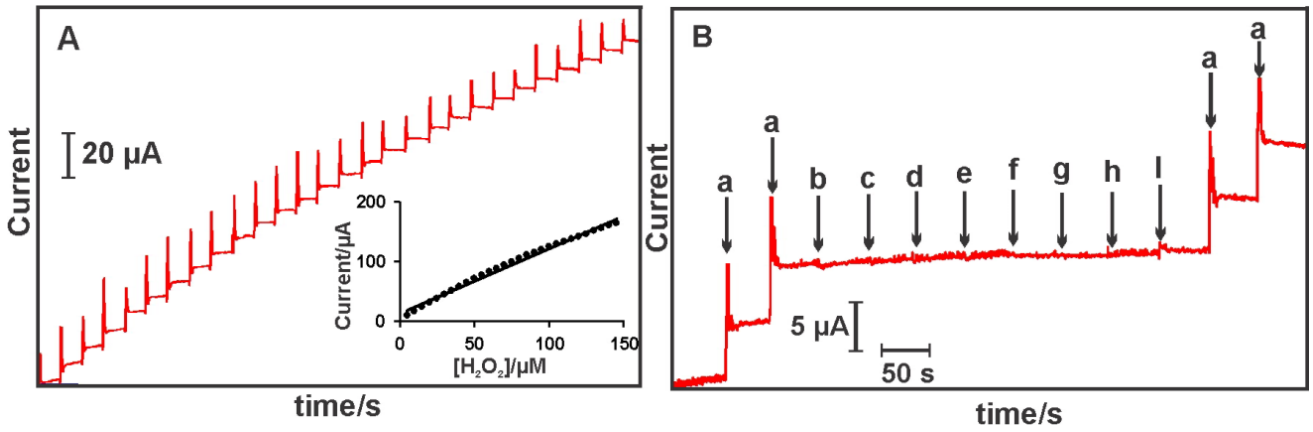

Figure 3. (A) Amperometric i–t response of MoS_2/GR-MWCNTs film modified rotating GCE upon sequential addition of 5 μM H_2O_2 into phosphate buffer (pH 7) at the rotation speed of 1500 RPM. E_{app} = – 0.45 V. Inset: Plot of I_p vs [H_2O_2]. (B) Amperometric i–t response of MoS_2/GR-MWCNTs film modified rotating GCE upon addition of 5 μM H_2O_2 (a) and externally added interferents dopamine, ascorbic acid, uric acid and glucose into phosphate buffer (pH 7) at the rotation speed of 1500 RPM.

3.4 Selectivity, stability, repeatability and reproducibility

Selectivity of the sensor to the determination of H_2O_2 has been investigated in the presence of common interfering agents. Fig. 3B displays the amperometric responses of the described sensor for 100 μM H_2O_2 (a) 0.1 mM (b) and 0.2 mM (c) dopamine, 0.1 mM (d) and 0.2 mM (e) ascorbic acid, 0.1 mM (f) and 0.2 mM (g) uric acid and 0.1 mM (h) and 0.2 mM (i) glucose. Well defined response was observed for H_2O_2; however, no notable responses were observed for the tested interfering species. Besides, well defined response was observed for H_2O_2 in the solution coexisting with aforementioned interferences revealed the excellent selectivity of the MoS_2/GR-MWCNTs to determine H_2O_2.

In order to determine storage stability of the MoS_2/GR-MWCNTs, its H_2O_2 detection perfomance was monitored every day. During one month storage period, the fabricated modified

electrode retained 91.55% of initial response current which revealing good storage stability. Repeatability and reproducibility of the proposed sensor was evaluated in phosphate buffer (pH 7) containing 50 μM H_2O_2. The sensor exhibits appreciable repeatability with relative standard deviation (R.S.D) of 3.78% for five repeatitive measurements which were carried out using single MoS_2/GR-MWCNTs/GCE. In addition, the sensor exhibits apprecible reproducibility with R.S.D of 3.83% for five independent measurments carried out at five different MoS_2/GR-MWCNTs/GCEs.

3.5 Real sample analysis

Practical applicability of the MoS_2/GR-MWCNTs/GCE was demonstrated in human serum sample. First, 2 ml serum sample was diluted to 10 ml by adding phosphate buffer (pH 7). Next, amperometry experiments were carried out using MoS_2/GR-MWCNTs/GCEs and following similar optimized experimental conditions. The found and recovery values are in acceptable range. Hence, the MoS_2/GR-MWCNTs/GCEs could be applicable for the real-time H_2O_2 sensing applications.

Table 1 Real-time determination of H_2O_2 in human serum sample using MoS_2/GR-MWCNTs film modified electrode

Sample	Added/μM	Found/μM	Recovery/%	*RSD/%
Human serum	10 μM	10.41 μM	104.1	3.73
	20 μM	20.52 μM	102.6	3.38

* Relative Standard Deviation of 3 individual measurements

4. CONCLUSIONS

In summary, we successfully prepared MoS_2/GR-MWCNTs nanocomposite through simple hydrothermal method. The composite was fully characterized by SEM, EDX and electrochemical methods. MoS_2/GR-MWCNTs/GCE exhibited excellent electrocatalytic ability to the reduction of H_2O_2. The fabricated amperometric sensor exhibited wide linear range (5 μM–145 μM), low detection limit (0.83 μM) and high sensitivity (5.184 μAμM cm^{-2}) for the determination of H_2O_2. Moreover, the sensor displayed appreciable stability and repeatability, reproducibity. The sensor holds great promise for real-time sensing application of H_2O_2 in biological samples. The MoS_2/GR-MWCNTs nanocomposite hold great potential for the fabrication of electrochemical sensors attributed to its large surface area, high conductivity, porosity, biocompatibility and stability.

ACKNOWLEDGEMENT
This work was supported by the Ministry of Science and Technology, Taiwan (Republic of China).

References

1. J. Wilson, A. Yoffe, *Adv. Phy.*, 18 (1969) 193.
2. B. Hinnemann, P.G. Moses, J. Bonde, K.P. Jørgensen, J.H. Nielsen, S. Horch, I. Chorkendorff, J.K. Nørskov, *J. Am. Chem. Soc.*, 127 (2005) 5308.
3. J. Xie, H. Zhang, S. Li, R. Wang, X. Sun, M. Zhou, J. Zhou, X.W.D. Lou, Y. Xie, *Adv. Mater.*, 25 (2013) 5807.
4. C. Tan, H. Zhang, *Chem. Soc. Rev.*, 44 (2015) 2713.
5. V. Mani, B. Dinesh, S.-M. Chen, R. Saraswathi, *Biosens. Bioelectron.*, 53 (2014) 420.
6. K.-Y. Hwa, B. Subramani, *Biosens. Bioelectron.*, 15 (2014) 127.
7. V. Mani, B. Devadas, S.-M. Chen, *Biosens. Bioelectron.*, 41 (2013) 309.
8. V. Mani, S.-M. Chen, B.-S. Lou, *Int. J. Electrochem. Sci*, 8 (2013) 11641.
9. Y. Yan, B. Xia, Z. Xu, X. Wang, *ACS Catal.*, 4 (2014) 1693.
10. S. Wi, H. Kim, M. Chen, H. Nam, L.J. Guo, E. Meyhofer, X. Liang, *ACS nano*, 8 (2014) 5270.
11. K. Chang, W. Chen, *Chem. Commun.*, 47 (2011) 4252.
12. L. Cao, S. Yang, W. Gao, Z. Liu, Y. Gong, L. Ma, G. Shi, S. Lei, Y. Zhang, S. Zhang, *Small*, 9 (2013) 2905.
13. Y. Yan, X. Ge, Z. Liu, J.-Y. Wang, J.-M. Lee, X. Wang, *Nanoscale*, 5 (2013) 7768.
14. H. Hwang, H. Kim, J. Cho, *Nano lett.*, 11 (2011) 4826.
15. X.-Y. Xu, Z.-Y. Yin, C.-X. Xu, J. Dai, J.-G. Hu, *Appl. Phy. Lett.*, 104 (2014) 033504.
16. D.H. Youn, S. Han, J.Y. Kim, J.Y. Kim, H. Park, S.H. Choi, J.S. Lee, *ACS nano*, 8 (2014) 5164.
17. G. Sun, X. Zhang, R. Lin, J. Yang, H. Zhang, P. Chen, *Angew. Chem. Int. Ed*, 127 (2015) 4734.
18. N. Lingappan, N.H. Van, S. Lee, D.J. Kang, *J. Power Sources*, 280 (2015) 39.
19. J.Y. Lin, A.L. Su, C.Y. Chang, K.C. Hung, T.W. Lin, *ChemElectroChem*, 2 (2015) 720.
20. Y. Shi, Z. Liu, B. Zhao, Y. Sun, F. Xu, Y. Zhang, Z. Wen, H. Yang, Z. Li, *J. Electroanal. Chem.*, 656 (2011) 29.
21. A.A. Ensafi, M. Jafari-Asl, N. Dorostkar, M. Ghiaci, M.V. Martínez-Huerta, J. Fierro, *J. Mater. Chem, B*, 2 (2014) 706.
22. K. Yamamoto, T. Ohgaru, M. Torimura, H. Kinoshita, K. Kano, T. Ikeda, *Anal. Chimi. Acta*, 406 (2000) 201.
23. B. Dinesh, V. Mani, R. Saraswathi, S.-M. Chen, *RSC Adv.*, 4 (2014) 28229.
24. B. Devadas, V. Mani, S.-M. Chen, *Int. J. Electrochem. Sci.*, 7 (2012) 8064.
25. W.S. Hummers Jr, R.E. Offeman, *J. Am. Chem. Soc.*, 80 (1958) 1339.
26. L. Qiu, X. Yang, X. Gou, W. Yang, Z.F. Ma, G.G. Wallace, D. Li, *Chem. Eur. J.*, 16 (2010) 10653.
27. R. Devasenathipathy, V. Mani, S.-M. Chen, *Talanta*, 124 (2014) 43.
28. B. Wang, J. Zhang, G. Cheng, S. Dong, *Anal. Chim. Acta*, 407 (2000) 111.
29. V. Mani, R. Devasenathipathy, S.-M. Chen, S.-F. Wang, P. Devi, Y. Tai, *Electrochim. Acta*, 176 (2015) 804.
30. S.A. Kumar, S.-M. Chen, *J. Mol. Cat. A: Chem.*, 278 (2007) 244.
31. Y. Ye, T. Kong, X. Yu, Y. Wu, K. Zhang, X. Wang, *Talanta*, 89 (2012) 417.